Catalysis Letters 36 (1996) 129–133

Platinum promoted zirconia–sulfate catalysts: one-pot preparation, physical properties and catalytic activity

M. Signoretto, F. Pinna, G. Strukul

Department of Chemistry, University of Venice, 30123 Venice, Italy

G. Cerrato and C. Morterra

Department of Inorganic, Physical and Materials Chemistry, University of Turin, 10125 Turin, Italy

Received 10 July 1995; accepted 22 September 1995

A new innovative methodology for the single-stage preparation of ZrO_2–SO_4 and Pt/ZrO_2–SO_4 catalysts is reported, based on the sol–gel technique. Catalysts are characterized by analysis, XRPD, BET and IR methods and are tested in the isomerization of butane.

Keywords: platinum; zirconia–sulfate; XRPD; BET; IR; isomerization; butane

1. Introduction

The use of zirconia–sulfate is attracting increasing interest in the literature because of the superacidic properties induced in these materials by the presence of SO_4^{2-} [1–6] that have been exploited in a variety of reactions, giving interesting results particularly in the hydroisomerization of alkanes [3,7,8]. It has also been observed that the addition of metals such as Fe–Mn [9–12], or Pt [1,13–16] greatly enhances the activity and the stability of these catalysts on stream.

To date, the system Pt/ZrO_2–SO_4 has been the most commonly studied, the role of the metal in the promotion of the catalytic performance being still a matter of debate [17,18]. Common feature in the preparation of these catalysts is a stepwise procedure consisting in the impregnation of aqueous H_2SO_4 or $(NH_4)_2SO_4$ on previously precipitated $Zr(OH)_4$, followed by drying and subsequent impregnation with H_2PtCl_6 solutions. Final operation is a calcination step at a temperature of about 600°C. This relatively complex set of operations can lead to the formation of samples with different characteristics, which may be at the origin of the different interpretations proposed for the nature of Pt and its role in the catalytic performance [17,18].

In the attempt to overcome some of these problems and find a more easily reproducible and reliable way to the preparation of this class of catalysts, in this paper we report some preliminary results in the synthesis of Pt/ZrO_2–SO_4 catalysts through a one-pot preparation procedure that is based essentially on sol–gel technology. While this work was in preparation, the same approach has been interestingly applied to the synthesis of ZrO_2–SO_4 catalysts [19].

2. Experimental

Preparation of the samples: In a conical flask were placed *i*-PrOH (100 ml), H_2SO_4 (96%, 0.8 ml), $H_2PtCl_6 \cdot 6H_2O$ (0.16 g) dissolved in *i*-PrOH (20 ml) and 70% $Zr(OPr)_4$ solution (36.8 ml). To this solution, a mixture of *i*-PrOH (60 ml) and H_2O (8.4 ml) was slowly added dropwise with stirring. When the addition was complete, the resulting mixture was stirred vigorously for 15 min and then left aside overnight at room temperature. When preparing ZrO_2–SO_4 samples, the addition of the H_2PtCl_6 solution was omitted. In the various samples, the amount of sulfuric acid used was changed according to the nominal SO_4^{2-} contents indicated in table 1.

Samples differ with respect to the solvent evaporation procedure. Xerogels were obtained by simply removing the solvent in vacuo (10^{-2} Torr) at room temperature. Aerogels were obtained as follows. The wet gel, obtained according to the above procedure, was placed in a 2 ℓ autoclave and covered with *i*-PrOH (450 ml). After flushing with N_2, the mixture was slowly heated (2.6°C/min) up to 250°C. After stabilizing the maximum temperature and pressure (60 bar) for 1 h, the solvent was slowly removed while the temperature was slightly increased to compensate for the pressure drop. Once the solvent was completely removed, the autoclave was flushed with N_2 and cooled down to room temperature.

Samples were calcined in air (30 ml/min) for 3 h at the temperature indicated in table 1 and then reduced in H_2 (30 ml/min) for 2 h at 300°C.

Quantitative determination of sulfates was performed by ion chromatography. Details on the experimental procedure are reported elsewhere [20].

Table 1
Physical parameters of the samples

Sample	Nominal SO_4^{2-} (wt%)	Found SO_4^{2-} (wt%)	T_{calc} (°C)	BET (m^2/g)	Cryst. phase composition
ZrO_2–SO_4(x)	17	2.7	550	88	T
ZrO_2–SO_4(a1)	17	6.4	600	140	T + 30% M
ZrO_2–SO_4(a2)	12.5	5.5	600	118	T
Pt/ZrO_2–SO_4(a2) [a]	12.3	6.1	600	143	T

[a] Pt 1.06 wt%.

XRPD analysis was performed using a Philips vertical goniometer connected with a highly stabilized generator. Cu Kα Ni-filtered radiation, a graphite monochromator and a proportional counter with a pulse height discriminator were used. The peak intensities were measured step by step (0.05° in 2θ) in several runs for a fixed time of 100 s.

BET surface areas were determined with N_2 at −196°C on a Carlo Erba 1900 Sorptomatic apparatus.

FTIR spectra were obtained at 2 cm^{-1} resolution with a Bruker IFS 113v spectrometer, equipped with MCT cryodetector adopting a strictly in situ configuration. All samples employed for IR measurements were in the form of thin layer deposition, prepared following a procedure described elsewhere [5,6].

Catalytic activity tests in the isomerization of *n*-butane were performed in a glass tubular reactor (200 mm long, 8 mm i.d.) externally heated by an oven. The temperature was controlled with a thermocouple immersed in the catalyst bed. The reaction was carried out at 250°C and atmospheric pressure by feeding (30 ml/min) a mixture of *n*-butane, hydrogen and helium ($H_2/C_4H_{10}/He = 6/1/0.4$). Prior to the reaction, the Pt-containing catalyst (1.5 g) was treated in a hydrogen stream (30 ml/min) at 300°C for 30 min. The other catalysts were activated in air (30 ml/min) at 450°C for 2 h. Isobutane was analyzed on line by gas-chromatography. Reaction rates were defined as mol isobutane formed per mol SO_4 in the sample per unit time.

3. Results and discussion

The application of sol–gel methods for the synthesis of the catalysts described here was exploited in four different cases: three ZrO_2–SO_4 samples and one Pt-containing sample. The basic idea is to add to the solution containing $Zr(OPr)_4$ an appropriate amount of H_2SO_4, which is used therefore as catalyst for both the hydrolysis and subsequent polycondensation of the $Zr(OH)_4$ sol to give the final gel. In fact, it is well known that acid or basic catalysis is generally required in sol–gel technology [21]. Where Pt is present, the addition of the H_2PtCl_6 solution takes place together with H_2SO_4 prior to gel formation. The resulting gels can be either dried at room temperature through an evaporation process in vacuo (xerogel) or via extraction of the solvent under supercritical conditions (aerogel). The Pt-containing sample was prepared only through the latter method.

Data on the composition of the samples are reported in table 1. As can be seen, both the nominal amount of sulfur introduced and the one actually present in the final materials are reported. This is an important analytical parameter that in most of previous reports on zirconia–sulfate has been overlooked, although it is known that much of the sulfate introduced in the preparation step is lost upon the thermal treatment necessary to prepare the active catalysts and that the activity of the latter is strongly dependent on the amount of residual sulfate groups.

It has to be pointed out that the specific analytical procedure [20] leads to extraction of surface sulfate groups, although these were found not to differ from the total sulfate groups [20]. As can be seen from table 1, a comparison between the amount of SO_4^{2-} introduced and the value found by analysis, indicates that in the samples prepared by aerogel the loss of sulfate upon calcination is less pronounced and leads to final contents that are approximately similar, independently of the initial amount of sulfate and the presence of platinum. Equally similar (and independent of Pt) is the surface area of the samples, with the consequence that the surface density of sulfate groups is approximately the same for all catalysts (~ 3 SO_4^{2-} groups/nm^2). In the sample prepared by xerogel, despite the much lower sulfate content, the surface density of sulfate groups is not very much different (2.3 SO_4^{2-} groups/nm^2) since the surface area of the sample is also lower with respect to the other samples. This feature is very common when comparing aerogels and xerogels and is associated in the latter with the collapse of the structure of the gel primary particles occurring when the solvent is evaporated under vacuum. The use of supercritical conditions in solvent evaporation leads to larger, porous primary particles that are also very stable during the calcination process resulting in a larger surface area in the final solid [22].

The use of strongly acidic conditions for the addition of H_2PtCl_6 in the starting reaction mixture should prevent the precipitation of hydrous oxides of Pt. It can be reasonably assumed that Pt remains mainly dissolved in the solvent until the evaporation step, when it is probably deposited on the surface of the primary oxide particles similarly to a traditional impregnation method.

However, it seems important to recognize that both SO_4^{2-} and Pt may be partly encapsulated in the bulk during gel formation and may not necessarily be surface species due to the mild activation treatment, although it is known that bulk SO_4^{2-} migrates on the surface upon crystallization of the material [19].

Standard XRPD analysis indicates that the sample prepared with the xerogel technique has a completely tetragonal crystal phase composition after calcination. Similarly, ZrO_2–SO_4(a2) is completely tetragonal, while ZrO_2–SO_4(a1) contains also ~ 30% monoclinic phase. Indeed, samples prepared by aerogel are already crystalline prior to calcination and their crystal phase composition seems almost unaffected by heat treatment (see for example fig. 1). This was unexpected, especially in view of the report of Ward and Ko [19] who found, with a similar preparation technique, materials that remained amorphous up to 400°C independently of the amount of H_2SO_4 used. However, it has to be pointed out that the conditions employed for attaining supercritical temperature and pressure are quite different in the case of CO_2 and *i*-PrOH, i.e. 70°C and atmospheric pressure for the former and 250°C and 60 atm for the latter. In the present case, since the evaporation temperature is still far below the minimum temperature observed by Ward and Ko [19] to induce crystallinity in ZrO_2–SO_4, it seems that the high pressure may be proposed as the major factor responsible for the occurrence of crystallinity even at low temperature; however, this did not seem to affect the catalytic properties of the materials (vide infra).

Interestingly, in the region of the Pt 111 reflection, evidence for the formation of Pt metal in Pt/ZrO_2–SO_4(a2) is quite clear both before and, most of all, after calcination (fig. 2). Partial reduction of Pt before calcination might be due to the reducing properties of *i*-PrOH, especially at high temperature. Indeed, the reduction step seems unnecessary for the genesis of the catalyst, as the X-ray diffractogram remains the same.

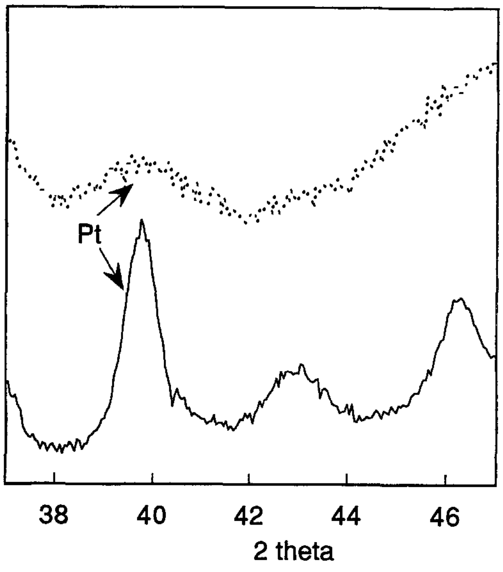

Fig. 2. X-ray diffraction patterns relative to Pt/ZrO_2–SO_4(a2) sample evidencing the Pt 111 reflection. Dotted line: before calcination. Solid line: after calcination.

The IR spectral features of the surface sulfate groups on these materials are reported in fig. 3. All spectra have been recorded after a standard activation in vacuo at 400°C in order to get rid of the abundant hydrated layer and reproduce the conditions in which the catalytic tests have been carried out. After this thermal treatment, surface sulfates reach the so-called covalent configuration, in which the ν_{S-O} band lies in the 980–1030 cm^{-1} range.

Little, but not null, differences are evidenced in the

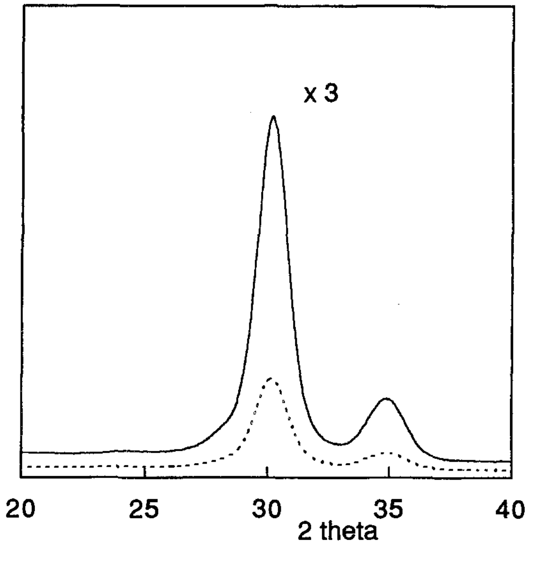

Fig. 1. X-ray diffraction profile for ZrO_2–SO_4(a2) evidencing the tetragonal phase. Dotted line: before calcination. Solid line: after calcination. The scaling factor is to avoid superimposition of the individual curves.

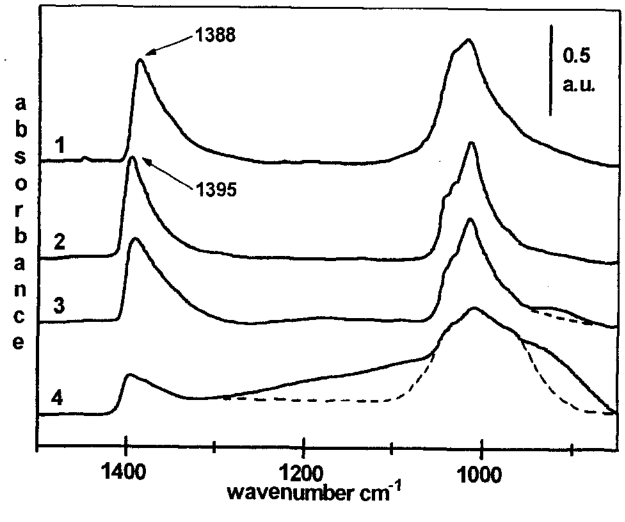

Fig. 3. Differential (absorbance) IR spectra in the 1500–850 cm^{-1} region relative to the different samples activated at 400°C: (1) Pt/ZrO_2–SO_4(a2); (2) ZrO_2–SO_4(a2); (3) ZrO_2–SO_4(a1); (4) ZrO_2–SO_4(*x*).

spectra relative to the Pt/ZrO_2–SO_4(a2) sample and the parent ZrO_2–SO_4(a2): in particular the $\nu_{S=O}$ band in the former is positioned at lower ν with respect to the latter and the ratio among the various components of the ν_{S-O} envelope is appreciably altered. As for the ZrO_2–SO_4(a1) and ZrO_2–SO_4(x) specimens, some peculiarities can be noticed with respect to the reference ZrO_2–SO_4(a2) system: the ZrO_2–SO_4(x) system (see for instance curve 4 in fig. 3) is characterized by a broader envelope in the low ν frequency range, with a huge component absorbing in the 870–970 cm^{-1} region, and a very broad absorption in the 1050–1250 cm^{-1} region. The former band could be ascribed to the ν_{S-O} mode of SO_x species, where either a different structure or a sulfur atom with an oxidation state lower than 6+ is present. The latter absorption is most likely characteristic of the symmetric vibration(s) of strongly coupled O=S=O species [23,24]. The ZrO_2–SO_4(a1) sample is virtually equivalent to the ZrO_2–SO_4(a2) reference, as it shows only one extra component positioned at ~ 950 cm^{-1}, the assignment of which is reported above for the ZrO_2–SO_4(x) sample. Overall, the spectra of fig. 3 indicate that the sulfate spectral features, especially those of the sulfates in the covalent configuration, are highly sensitive to the preparation procedure.

The acidity of the samples has been tested by pyridine adsorption and seemed to be the same both with and without Pt present and very similar to that found for samples prepared with the traditional method [5]. The Lewis/Brønsted sites ratio is strongly dependent on the calcination temperature and, mostly, on the activation temperature and under the conditions reported in fig. 3, Lewis acid sites largely exceed Brønsted sites.

The Lewis acidity of these systems has been tested also through the adsorption of carbon monoxide at room temperature (RT). In these conditions, CO is able to reveal (i) the strongest fraction of coordinatively unsaturated surface Zr^{4+} sites (fig. 4) yielding bands at ν higher than that of the free CO gas molecule (2143 cm^{-1}); (ii) if present, coordinatively unsaturated Pt metal atoms/ions yielding bands at ν lower than that of the free CO gas molecule. Needless to say, the intensity of the CO band is a semiquantitative measure of the concentration of the surface sites interacting at RT with CO.

It is worth noting that CO does not form any carbonyl species with Pt^0 (curve 1 in fig. 4) and it starts interacting with CO only after a thermal activation/oxidation process (curve 1′ in fig. 4). The ν_{CO} of this weak species lies at ~ 2080 cm^{-1}, indicating a species in which a partial back-donation from the π orbital of Pt^0 is present. If we compare the intensity and the breadth of this CO band with that obtained in the same conditions for a non-sulfated Pt/ZrO_2 system (curve 1* in fig. 4), it is evident that the Pt^0 species present on Pt/ZrO_2–SO_4(a2) are either not available or only partially available to CO; besides, no evidence for the presence of Pt^{n+} species is ever observed. This behavior is most unexpected and will be discussed elsewhere [25].

As for the CO species formed on coordinatively unsaturated Zr^{4+} surface centers, the spectra of fig. 4 show that the strong Lewis acidity due to these centers is quite high (see the strong band of σ-coordinated CO at 2196 cm^{-1}) and that no appreciable differences are induced by the various preparation procedures.

The activity of the catalysts in the isomerization of n-butane is shown in figs. 5 and 6. Reactions were carried out at 150°C in the absence of H_2 and as expected the conversion declines slowly as a consequence of a deactivation process. A comparison of the rates calculated on a per site basis between ZrO_2–SO_4(x) and ZrO_2–SO_4(a1)

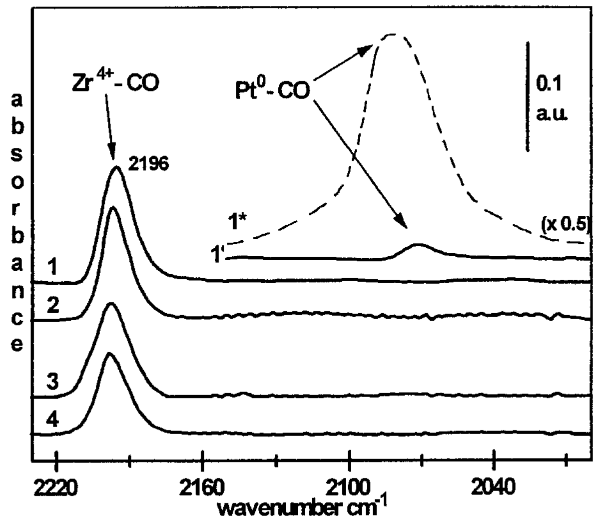

Fig. 4. Differential (absorbance) IR spectra in the 2225–2050 cm^{-1} region relative to the adsorption of 100 Torr CO at room temperature on the different systems: (1*) non-sulfated Pt/ZrO_2 reference system; (1′) Pt/ZrO_2–SO_4(a2) activated/oxidized at 400°C; (1) Pt/ZrO_2–SO_4(a2); (2) ZrO_2–SO_4(a2); (3) ZrO_2–SO_4(a1); (4) ZrO_2–SO_4(x).

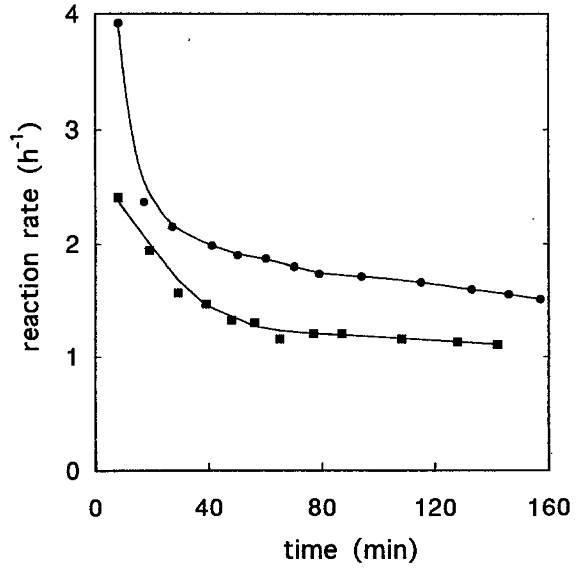

Fig. 5. Rate vs. time plot for the catalytic isomerization of n-butane at 150°C. Circles: ZrO_2–SO_4(a1); squares: ZrO_2–SO_4(x).

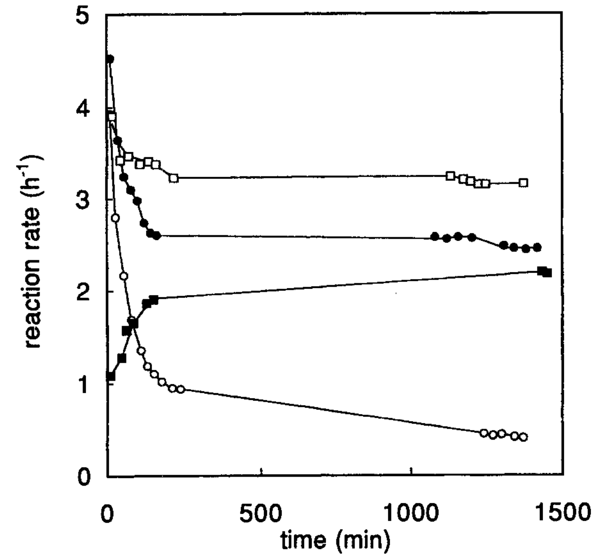

Fig. 6. Rate vs. time plot for the catalytic isomerization of *n*-butane at 250°C in the presence of hydrogen. Squares: Pt/ZrO$_2$–SO$_4$(a2); circles: ZrO$_2$–SO$_4$(a2). Open symbols: H$_2$/butane 1/1; filled symbols: H$_2$/butane 6/1.

indicates that the latter sample is significantly more active. The differences are even higher in terms of conversion: for example after 120 min conversions are 5% for ZrO$_2$–SO$_4$(x) and 16% for ZrO$_2$–SO$_4$(a1). Indeed, the activity computed in fig. 5 for ZrO$_2$–SO$_4$(a1) might be partly reduced by the fact that the sample is $\sim$ 30% monoclinic at variance with ZrO$_2$–SO$_4$(x) that is purely tetragonal. The association of the catalytic activity of these materials with the presence of the tetragonal crystal phase is well known [26]. Compared to previous samples [19] prepared in a similar manner, the present catalysts appear to be significantly more active even in the absence of H$_2$.

A comparison of the effect of the presence of Pt on the catalytic activity is shown in fig. 6, where ZrO$_2$–SO$_4$(a2) and Pt/ZrO$_2$–SO$_4$(a2) are reported. Reactions were carried out at 250°C in the presence of H$_2$ and were monitored for at least 24 h. As is known [27], the addition of H$_2$ in the feed increases the stability of ZrO$_2$–SO$_4$ catalysts and, indeed, the activity and stability of our sample prepared by aerogel is greatly increased when the H$_2$/butane ratio increases from 1/1 to 6/1. The addition of Pt seems to have no influence on the activity of the catalyst under high H$_2$/butane ratio. After 24 h the difference between ZrO$_2$–SO$_4$(a2) and Pt/ZrO$_2$–SO$_4$(a2) is negligible. Lowering the H$_2$/butane ratio to 1/1 leads in the case of Pt/ZrO$_2$–SO$_4$(a2) to an increase of the activity by a factor of about 1.5, while maintaining the stability of the catalyst. The effect is dramatic if compared to the behavior of ZrO$_2$–SO$_4$(a2) under the same conditions (fig. 6).

Acknowledgement

Thanks are expressed to CNR (Rome) and MURST (Rome) for financial support.

References

[1] K. Arata, Adv. Catal. 37 (1990) 165.
[2] M. Hino, S. Kobayashi and K. Arata, J. Am. Chem. Soc. 101 (1979) 6439.
[3] M. Hino and K. Arata, J. Chem. Soc. Chem. Commun. (1980) 851.
[4] A. Clearfield, G.P.D. Serrete and A.H. Khazi-Syed, Catal. Today 20 (1994) 295.
[5] C. Morterra, G. Cerrato, F. Pinna, M. Signoretto and G. Strukul, J. Catal. 149 (1994) 181.
[6] F. Pinna, M. Signoretto, G. Strukul, G. Cerrato and C. Morterra, Catal. Lett. 26 (1994) 339.
[7] J.M. Parera, Catal. Today 15 (1992) 481.
[8] P. Nascimento, C. Akratopoulou, M. Oszagyan, G. Coudurier, C. Travers, J.F. Joly and J.C. Vedrine, in: *New Frontiers in Catalysis,* Proc. 10th Int. Congr. on Catalysis, Vol. B, eds. L. Guczi, F. Solymosi and P. Tétényi (Akadémiai Kiadó, Budapest, 1993) p. 1185.
[9] C.-Y. Hsu, C.R. Heimbruch, C.T. Armes and B.C. Gates, J. Chem. Soc. Chem. Commun. (1992) 1645.
[10] T.-K. Cheung, J.L. d'Itri and B.C. Gates, J. Catal. 151 (1995) 464.
[11] V. Adeeva, G.D. Lei and W.M.H. Sachtler, Appl. Catal. A 118 (1994) L-11.
[12] V. Adeeva, J.W. de Haan, J. Jänchen, G.D. Lei, V. Schünemann, L.J.M. van de Ven, W.M.H. Sachtler and R.A. van Santen, J. Catal. 151 (1995) 364.
[13] K. Ebitani, J. Konishi and H. Hattori, J. Catal. 130 (1991) 257.
[14] K. Ebitani, H. Konno, T. Tanaka and H. Hattori, J. Catal. 135 (1992) 60.
[15] B.H. Davis, R.A. Keogh and R. Srinivasan, Catal. Today 20 (1994) 219.
[16] T. Yamaguchi, Appl. Catal. 61 (1990) 1.
[17] A. Sayari and A. Dicko, J. Catal. 145 (1994) 561.
[18] K. Ebitani, H. Konno, T. Tanaka and H. Hattori, J. Catal. 143 (1993) 322.
[19] D.A. Ward and E.I. Ko, J. Catal. 150 (1994) 18.
[20] C. Sarzanini, G. Sacchero, F. Pinna, M. Signoretto, G. Cerrato and C. Morterra, J. Mater. Chem. 5 (1995) 353.
[21] C.J. Brinker and G.W. Scherer, *Sol–Gel Science: the Physics and Chemistry of Sol–Gel Processing* (Academic Press, New York, 1990) chs. 1, 2.
[22] C.J. Brinker and G.W. Scherer, *Sol–Gel Science: the Physics and Chemistry of Sol–Gel Processing* (Academic Press, New York, 1990) chs. 8, 9.
[23] C. Morterra, G. Cerrato, C. Emanuel and V. Bolis, J. Catal. 142 (1993) 349.
[24] C. Morterra, G. Cerrato, F. Pinna and M. Signoretto, J. Catal., in press.
[25] C. Morterra, G. Cerrato, F. Pinna, M. Signoretto and G. Strukul, to be published.
[26] F.R. Chen, G. Coudurier, J.-F. Joly and J.C. Vedrine, J. Catal. 143 (1993) 616.
[27] F. Garin, D. Andriamasinoro, A. Abdulsamad and J. Sommer, J. Catal. 131 (1991) 199.